Modelling three-dimensional directivity of sound scattering by Antarctic krill: progress towards biomass estimation using multibeam sonar

George R. Cutter, Josiah S. Renfree, Martin J. Cox, Andrew S. Brierley, and David A. Demer

Cutter, G. R., Renfree, J. S., Cox, M. J., Brierley, A. S., and Demer, D. A. 2009. Modelling three-dimensional directivity of sound scattering by Antarctic krill: progress towards biomass estimation using multibeam sonar. – ICES Journal of Marine Science, 66: 1245–1251.

Target strength (*TS*) estimation is a principal source of uncertainty in acoustic surveys of Antarctic krill (*Euphausia superba*). Although *TS* is strongly dependent on krill orientation, there is a paucity of information in this regard. This paper considers the potential for narrow-bandwidth, multibeam-echosounder (MBE) data to be used for estimating the orientations of krill beneath survey vessels. First, software was developed to predict MBE measurements of the directivity patterns of acoustic scattering from individual or aggregated krill in any orientation. Based on the distorted-wave, Born approximation model (DWBA), scattering intensities are predicted vs. MBE angles for specified distributions of krill orientations (pitch, roll, and yaw angles) and swarm densities. Results indicate that certain distributions of orientations, perhaps indicative of particular behaviour, should be apparent from the sonar data. The model results are compared with measurements on krill made using a 200-kHz MBE deployed from a small craft off Cape Shirreff, Livingston Island, Antarctica, in summer 2006. The stochastic DWBA model is then invoked to explain disparities between the model predictions and MBE measurements.

Keywords: Antarctic krill, directivity, incidence angle, multibeam sonar, orientation, target strength.

Received 11 August 2008; accepted 28 December 2008; advance access publication 18 March 2009.

G. R. Cutter, J. S. Renfree, and D. A. Demer: Southwest Fisheries Science Center, 8604 La Jolla Shores Drive, La Jolla, CA 92037, USA. M. J. Cox and A. S. Brierley: Gatty Marine Laboratory, School of Biology, University of St Andrews, Fife KY16 8LB, Scotland, UK. Correspondence to G. R. Cutter: tel: +1 858 546 5691; fax: +1 858 546 5656; e-mail: george.cutter@noaa.gov.

Introduction

High-frequency ($\geq$70 kHz) acoustic scattering from Antarctic krill (*Euphausia superba*) is highly directional. For example, the distorted-wave, Born-approximation model (DWBA; McGehee *et al.*, 1998) and the Stochastic DWBA model (SDWBA; Demer and Conti, 2003a; Conti and Demer, 2006) predict that the target strength (*TS*) of krill at 120 kHz is 20 dB lower for a tilt angle $\theta = 15^\circ$ off the dorsal incidence than at $\theta = 0^\circ$. Consequently, the *TS* of krill at typical sonar frequencies can vary substantially, particularly for $\theta < 30^\circ$.

The orientations of *in situ* krill are variable and largely unknown. What is known about θ for krill was derived from measurements of *ex situ* krill and inferences from data on *in situ* krill. For krill hovering in an aquarium, Kils (1981) and Endo (1993) estimated $\theta = 45^\circ$ (s.d. $= 30^\circ$) and $\theta = 45^\circ$ (s.d. $= 20^\circ$), respectively. For krill swimming in a flume, Kils (1981) measured $\theta \approx 5$–30°, with the smaller angles corresponding to faster speeds. From acoustic observations, Chu *et al.* (1993) estimated $\theta \approx 0$–30° for swimming, encaged krill, whereas Demer and Conti (2005), Conti *et al.* (2005), and Conti and Demer (2006) estimated $\theta \approx 11$–15° (s.d. $= 4$–5°) for krill beneath a survey vessel. Lawson *et al.* (2006) estimated $\theta \approx 10^\circ$ (s.d. $= 60^\circ$; median $\theta = -0.5^\circ$) visually for krill passing through a towed, video plankton recorder. Most of these observations indicate that krill orientate head-up (positive θ) when at rest and are orientated nearly horizontal ($\theta \approx 0^\circ$) when swimming. Consequently, it must be assumed that krill in the wild can adopt any orientation, depending on their behaviour.

For acoustic surveys of krill conducted using a single-beam echosounder (SBE), θ modulates the incidence angle and hence the measured *TS*. Measurements of volume-backscattering strength ($S_v = TS + 10 \log N$, where N is the number of scatterers per cubic metre) are therefore also modulated by θ. Therefore, the generally unknown orientation of krill is a principal source of uncertainty in acoustic estimates of their density, abundance, and biomass. Better knowledge of krill orientations, particularly during acoustic observations, would constitute a major step towards reducing uncertainty in surveys with SBEs. Perhaps such information would also allow the use of multibeam echosounders (MBEs), that have swaths of 90–180°, for quantitative surveys of krill. At present, the multiple angles of incidence associated with the various beams make quantitative translation of echo intensity to numerical density essentially impossible.

Although some *TS* models of krill are parameterized for any incidence angle, only variations in *TS* vs. θ have yet been considered (Martin Traykovski *et al.*, 1998; McGehee *et al.*, 1998; Demer and Conti, 2003a). Distributions of θ have been estimated for krill by inverting *TS* models using broad-bandwidth (Martin Traykovski *et al.*, 1998) and multifrequency measurements of S_v (Chu *et al.*, 1993; Conti *et al.*, 2005; Demer and Conti, 2005; Conti and Demer, 2006). These methods are ineffective,

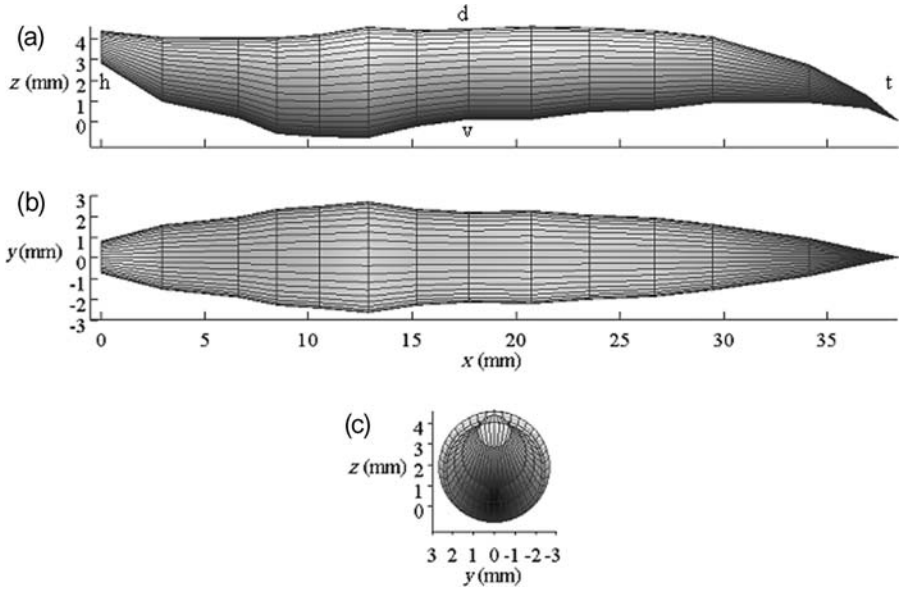

Figure 1. Three views of the shape used to represent a generic krill for the DWBA and SDWBA models; (a) left side, (b) dorsal, and (c) head. Labels in (a) indicate the dorsal ('d') and ventral ('v') surfaces, and the head ('h') and tail ('t') of the krill.

however, if the scattering-directivity pattern (SDP) is complicated or if the acoustic beam is non-vertical.

Krill can adopt any orientation because of natural behaviour, water motion, or reactions to the presence of a survey vessel as can fish (Gerlotto and Fréon, 1992; Soria *et al*., 1996; Gerlotto *et al*., 2004). The combination of krill orientations and the range of beam directions from a wide-swath MBE, or a motion-uncompensated SBE, means that krill could be insonified from any direction. Therefore, this study considers not only θ, but also any orientation resulting from the pitch, roll, and yaw of the krill, combined with variations in the direction of the acoustic beam. Here, the *TS* values for any incidence angle are modelled using the DWBA (McGehee *et al*., 1998), resulting in complete, three-dimensional, frequency-specific, SDPs for krill, similar to those produced for fish by Jech and Horne (2002) and Towler *et al*. (2003). Using the krill SDPs, and a simulation model of the MBE developed by Cutter and Demer (2007), distributions of scattering intensity are predicted for many beam directions and various distributions of krill orientations and aggregation densities. These simulation results are compared with MBE data. Although the work focuses on krill, the findings here are also relevant to surveys of any pelagic species conducted with MBEs and SBEs.

Table 1. Values of cylinder radii *a* used for the krill-shape model.

$a_{McGehee}$ (m)	a_{fat} (m)	*x* (m)	*y* (m)	*z* (m)
0.000	0.000	3.835×10^{-2}	0.000	0.000
2.147×10^{-4}	3.006×10^{-4}	3.686×10^{-2}	0.000	9.149×10^{-4}
6.525×10^{-4}	9.136×10^{-4}	$3.405 \times 10-^{2}$	0.000	1.792×10^{-3}
1.130×10^{-3}	1.581×10^{-3}	2.942×10^{-2}	0.000	2.455×10^{-3}
1.354×10^{-3}	1.895×10^{-3}	2.662×10^{-2}	0.000	2.437×10^{-3}
1.447×10^{-3}	2.026×10^{-3}	2.353×10^{-2}	0.000	2.455×10^{-3}
1.596×10^{-3}	2.235×10^{-3}	2.070×10^{-2}	0.000	2.306×10^{-3}
1.550×10^{-3}	2.170×10^{-3}	1.770×10^{-2}	0.000	2.250×10^{-3}
1.652×10^{-3}	2.313×10^{-3}	1.519×10^{-2}	0.000	2.054×10^{-3}
1.904×10^{-3}	2.666×10^{-3}	1.285×10^{-2}	0.000	1.848×10^{-3}
1.755×10^{-3}	2.457×10^{-3}	1.053×10^{-2}	0.000	1.690×10^{-3}
1.652×10^{-3}	2.313×10^{-3}	8.467×10^{-3}	0.000	1.690×10^{-3}
1.382×10^{-3}	1.934×10^{-3}	6.647×10^{-3}	0.000	2.063×10^{-3}
1.102×10^{-3}	1.542×10^{-3}	2.969×10^{-3}	0.000	2.474×10^{-3}
5.508×10^{-4}	7.711×10^{-4}	0.000	0.000	3.557×10^{-3}

The density contrast was $g = 1.0357$, and the sound-speed contrast $h = 1.0279$. The number of cylinders, N_{bcyl}, was 6, 10, 15, and 25 at frequencies 38, 70, 120, and 200 kHz, respectively.

Methods

Modelling krill shape

The DWBA was parameterized with a generic krill shape (Figure 1) comprising multiple, contiguous cylinders distributed along a curve (McGehee *et al*., 1998). Shape parameters include the cylinder radii *a* (m), the density contrast *g*, the sound-speed contrast *h*, and the locations of the centres of each cylinder *r*, in rectangular coordinates (Table 1). As in Demer and Conti (2003b, 2005) and Conti and Demer (2006), the radii (*a*) were 40% larger than those of the starved krill modelled in McGehee

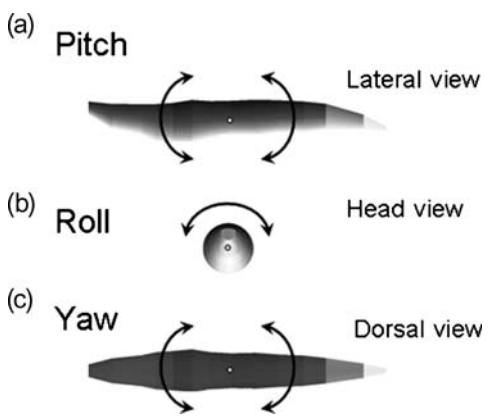

Figure 2. Definitions of pitch, roll, and yaw used in the simulations. A horizontal krill with the dorsal side upwards has zero pitch. Positive pitch corresponds to head-up rotations.

et al. (1998). The standard krill length, $L = 38.35$ mm, is from the front of the eyes to the tip of the telson. The number of cylinders, N_{bcyl}, varied with the acoustic frequency, as in Conti and Demer (2006).

Modelling SDPs

The DWBA was used to model krill SDPs for the commonly employed acoustic frequencies of 38, 70, 120, and 200 kHz. Following the reference frame and angle definitions in McGehee *et al.* (1998), the krill shapes were transformed, first by translating the central axis of the krill to the *x*-axis, then rotating the krill about that axis over 360° at 1° intervals. For each roll-angle interval, the model predicted *TS* for 1° intervals over 360° in the vertical plane. Therefore, *TS* data were modelled for all directions, and the results at each interval were combined to form the complete SDP.

SDPs were similarly generated for 120 and 200 kHz using the SDWBA. *TS* values were estimated for ten realizations with random phases and s.d. $(\phi) = 0.7070$ radians; see Demer and Conti (2003a, b) for details.

Modelling multibeam measurements

The 200-kHz SDPs calculated with both the DWBA and SDWBA were used in a simulation program (Cutter and Demer, 2007) to predict MBE measurements of scattering intensity from krill aggregations with specified densities (number per m^3 per beam) and orientation distributions, defined by the mean $\pm$ s.d. for normal angle distributions and the minima and maxima for uniform distributions. Krill orientations were controlled by three angles. The pitch describes rotation about the lateral axis of the krill, or head-up, tail-down motion; the roll describes rotation about the head–tail axis; and the yaw describes rotation about the vertical axis (Figure 2). In each simulation, the number of krill was varied from 25 to 50 per m^3. These densities were large enough to produce distributions with approximately normal pitch and uniform yaw. The same distributions of krill orientation were used for all beams. It was assumed that each krill was insonified on the beam axis, where the acoustic sensitivity is at a maximum. Outputs of the simulation included *TS* for each beam and each krill, and the mean and distribution of S_v, normalized to one animal per unit volume for the krill insonified by each beam. Hence, the model results can be adjusted to predict S_v for any number (N) of krill as the sum of the normalized S_v and $10 \log(N)$. Data were simulated for a subset (at intervals of 10°) of beams spanning an athwartships swath of 180° ($\pm$ 90° to each side of the vertical).

Multibeam data

A 200-kHz MBE (Kongsberg-Mesotech SM2000/SM20) was used to survey krill in shallow water (<200 m) off Cape Shirreff, Livingston Island, Antarctica (Cox *et al.*, in press) from 2 to 9 February 2006. The MBE was deployed from a small (6 m long) inflatable boat (Mark V Zodiac). The MBE has 128 beams spanning a 120° swath. The transmit power was 'medium', pulse duration was 825 μs, maximum range was 200 m, TVG was $20 \log R + 2 \alpha R$ (where R is the range and α the absorption coefficient). The raw data were recorded and gain compensation was applied during post-processing.

The S_v measurements from the MBE were calibrated (offset = −71.2 dB) against measurements made concurrently with a calibrated 200-kHz SBE (Simrad ES60; see Cox *et al.*, in press, for details). The S_v from krill swarms were exported from Echoview (Myriax, Hobart, Australia) for calculations of the mean and s.d. of S_v vs. beam direction as in Cutter and Demer (2007). These data were compared with patterns predicted by the simulation. Additionally, S_v vs. range and bearing were exported for all swarms identified using Echoview's school-detection routine in the multibeam module (Cox *et al.*, in press). A random set of 100 pings from these data was examined for patterns of S_v vs. beam direction.

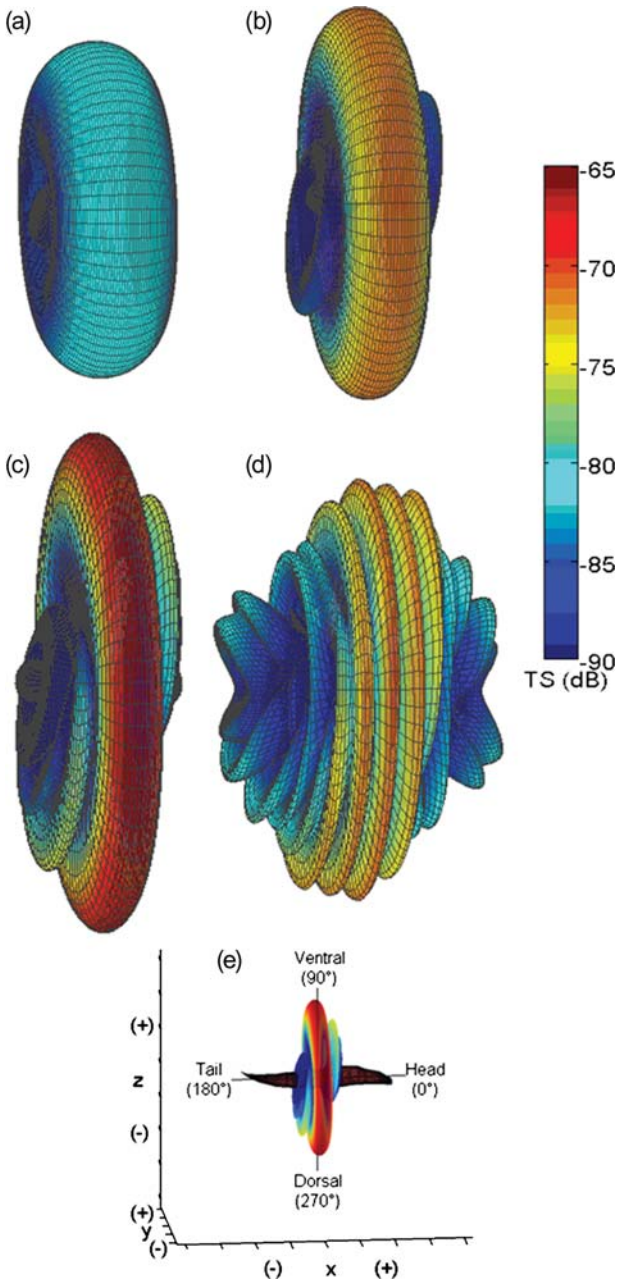

Figure 3. SDPs representing the *TS* (dB) for any beam-incidence angle about a krill (*E. superba*); results from the DWBA model for (a) 38 kHz, (b) 70 kHz, (c) 120 kHz, (d) 200 kHz, and (e) the krill shape depicted within the 120 kHz SDP illustrating the incidence directions.

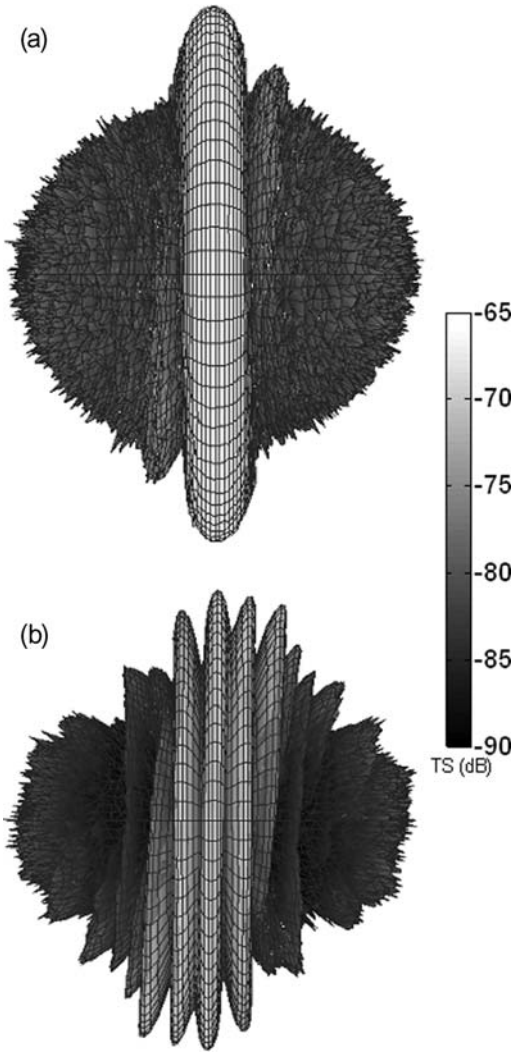

Figure 4. SDPs representing the *TS* (dB) for any beam-incidence angle about a krill (*E. superba*), resulting from the SDWBA model for (a) 120 kHz, and (b) 200 kHz.

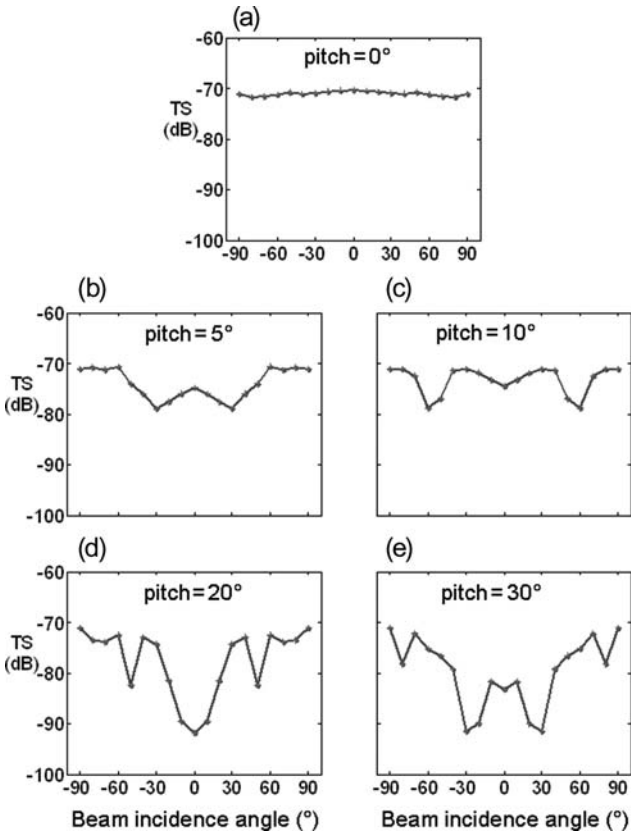

Figure 5. *TS* predicted by the multibeam-directivity model for 200 kHz, beam directions from −90° to 90°, and krill-pitch angles of (a) 0°, (b) 5°, (c) 10°, (d) 20°, and (e) 30°.

Results

Krill SDPs

SDPs based on the DWBA at 38, 70, 120, and 200 kHz were imaged three-dimensionally (Figure 3). The complexity and directivity increase with frequency. At 38 kHz, the SDP resembles a simple disc or compressed sphere, with a nearly circular main lobe ($TS \approx -$ 80 dB) in the plane defined by the lateral (y) and dorso-ventral (z) axes (Figure 3a). The SDPs at 70 and 120 kHz have a narrow main lobe and two (70 kHz; Figure 3b) to four (120 kHz; Figure 3c) side lobes, tilted in the y–z plane towards the head–tail axis. The SDP for 200 kHz has a very narrow main lobe and several narrow side lobes in close proximity to dorsal incidence, with peaks nearly equal to the main lobe (Figure 3d). Among these frequencies, krill *TS* was highest at 120 kHz with a peak value of −65.4 dB at dorsal incidence.

For comparison, the SDPs based on the SDWBA at 120 and 200 kHz are presented in Figure 4. The phase variations modelled in the SDWBA had little effect on the dorso-ventral scattering. However, the SDWBA predicted an increase in the *TS* observed from the head and tail directions and reduced directivity off the main lobes. These effects were most pronounced in the 120-kHz SDP, where the scattering was nearly uniform for all incidence angles away from the primary lobe, and include a more subtle, tilted secondary lobe.

Modelled multibeam measurements

The 200-kHz SDP from the DWBA was used to simulate measurements of S_v vs. beam direction for an MBE with 180° swath. The resulting S_v vs. pitch is displayed in Figure 5. When krill are horizontal and aligned with the ship, the MBE beams intersect the main lobe of the SDP at all incidence angles, resulting in a nearly constant *TS* of approximately −70 dB. If pitch = 5°, the S_v observed in the vertical beam changed by −5 dB; and by nearly −10 dB in the beams 30° to either side of the vertical.

To simulate MBE measurements of S_v at 200 kHz from a krill aggregation with a pitch distribution N(11°, 4°), as described by Conti and Demer (2006), and a uniform distribution of yaw, DWBA-SDPs representing 25 krill were insonified by each beam. The resulting mean S_v were 5–10 dB higher in the beams ±20° from the vertical compared with the outer beams. When the simulated pitch distribution was broader [e.g. N(11°, 24°)], the values of S_v were nearly equivalent, with approximately equal variance vs. beam direction (Figure 6).

Multibeam survey data

Various patterns of S_v vs. beam direction were apparent in the MBE data, but none was dominant. The observed patterns included nearly uniform, trending, alternating high and low, and occasionally an

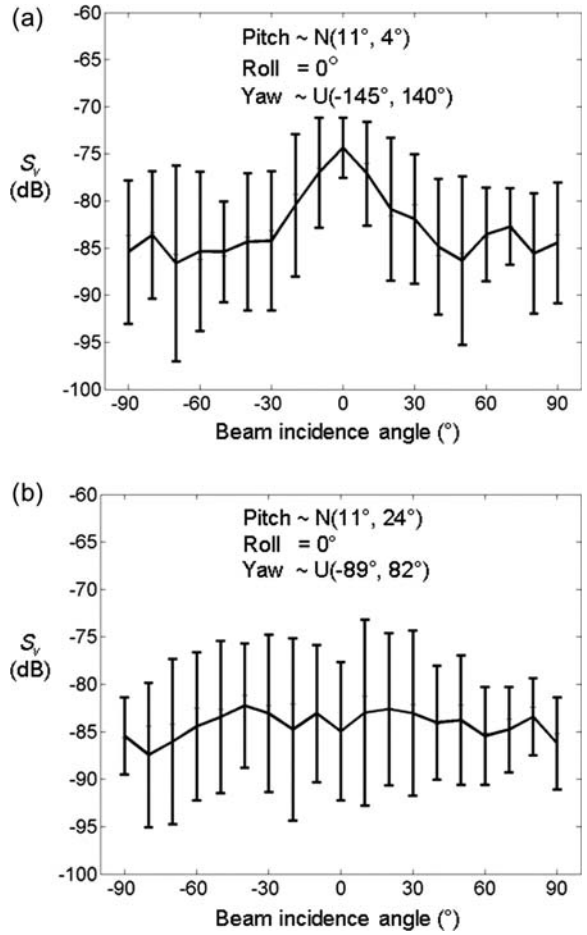

Figure 6. Target-strength distributions predicted by the multibeam-directivity model for 200 kHz and 25 krill per beam. The krill are orientated with uniform yaw and (a) pitch$\sim$N(11°, 4°), and (b) pitch$\sim$N(11°, 24°). The realized distributions of yaw were (a) $\sim$U($-145°$, 140°), and (b) $\sim$U($-89°$, 82°).

absence of krill in the beams at and near vertical incidence (Figure 7). The S_v vs. beam direction was variable, with S_v ranging $\pm 2-10$ dB from the mean value of each pattern (Figure 7). Trends and patterns of S_v vs. beam direction were evident in some pings, but none could be clearly matched to the simulation results. For example, the simulation predicted that for a mean pitch = 11°, S_v should be $\sim$5 dB lower for the vertical vs. outer beams when yaw = 0°, and higher in the near-vertical beams for non-zero, variable yaw. Lower S_v in near-vertical beams was apparent in at least one case, but this could not be attributed uniquely to yaw. The result could also have been caused by non-uniform krill density that could occur naturally or a reaction to the vessel.

Discussion

When surveying krill with an SBE at the common frequencies of 70, 120, and 200 kHz, *TS* and S_v are highly sensitive to small changes in pitch, but roll has negligible effect. However, when surveying with a high-frequency MBE, the pitch, roll, and yaw of krill are all important, because the SDPs are complex and the large swath insonifies the krill at many incidence angles.

For SBEs without motion compensation, the vessel's roll and pitch will result in non-vertical beams. The SDPs for krill at 70–200 kHz are most variable within $\pm 45°$ of dorsal-aspect incidence. Within a narrow range of beam directions ($\pm 15°$), *TS* of krill can vary by $\sim$10 dB (at 200 kHz), depending on the krill orientations. If a krill yaws a mere 15° off the vessel-track direction, and the beam direction varies from 0° to 15° because of vessel motion (for the SBE), or for that portion of an MBE swath, the measured *TS* can range from -70.4 to -81.7 dB. Therefore, krill yaw is important even for surveys with SBEs, particularly at frequencies >120 kHz.

The krill *TS* and the SDP depend on the animal size relative to the sound wavelength. The krill model used in this study was chosen to be consistent with the size of krill modelled in previous studies (McGehee *et al.*, 1988; Demer and Conti, 2003b). Demer and Conti (2003b) measured krill length-frequency distributions from $\sim$20 to 50 mm, with an overall mean of 31.6 mm (s.d. = 6.6 mm). Larger krill would probably have slightly higher mean *TS* values and somewhat more complicated SDPs at lower frequencies (<200 kHz). Similarly, the SDP of smaller krill at 200 kHz would probably have a simpler geometry, a lower directivity, and a lower mean *TS* averaged over all angles.

For krill orientated with pitch$\sim$N(11°, 4°) (Conti and Demer, 2006) and yaw$\sim$U($-149°$, 139°), the simulations based on the SDWBA at 200 kHz indicate an obvious pattern in the multibeam data (Figure 8). Specifically, measured scattering intensities should be nearly 8 dB higher for the near-vertical beams relative to the outer beams. This was not observed in the field data.

Many explanations are possible for the absence of the expected patterns in the MBE field data. For example, the pitch distribution might not be the N(11°, 4°) estimated by Conti and Demer (2006) for krill beneath a large vessel surveying at speed, or the krill might have been dispersed throughout each beam, as opposed to being only on the beam axes. That is, the MBE measurements were convolved with the beam patterns of each beam. A refinement of the simulation model should therefore account for beam-pattern effects. Alternatively, measurements with a fully calibrated MBE, particularly a split-beam instrument such as the Simrad ME70, could be deconvolved with the known beam patterns before comparison with the simulation results. Another hypothesis is that the krill changed their natural orientations or locations in vessel-avoidance reactions, as suggested by the swarms detected in the outer beams compared with those in the inner beams (Figure 7).

Non-uniform orientation distributions are difficult to estimate even for scatterers with high and known SDPs. Hence, the estimation of scatterers' orientation from narrowband MBE data requires restrictive conditions. However, concurrent multibeam and multifrequency split-beam measurement spanning 38–200 kHz could better constrain the problem and provide better estimates of scatterer' orientations.

Conclusions

If the orientation angles of the insonified krill are not known, the measured *TS* and S_v include large uncertainties. A calibrated MBE is not prerequisite to detect the S_v vs. beam-direction patterns associated with known consistent distributions of krill orientations. Therefore, krill orientations can be estimated from narrowband, multibeam data if all krill in an aggregation are orientated similarly across all beam directions, for example if krill are responding to a vessel in a predictable manner. However, the MBE must be calibrated to allow a quantitative comparison with a calibrated, split-beam SBE.

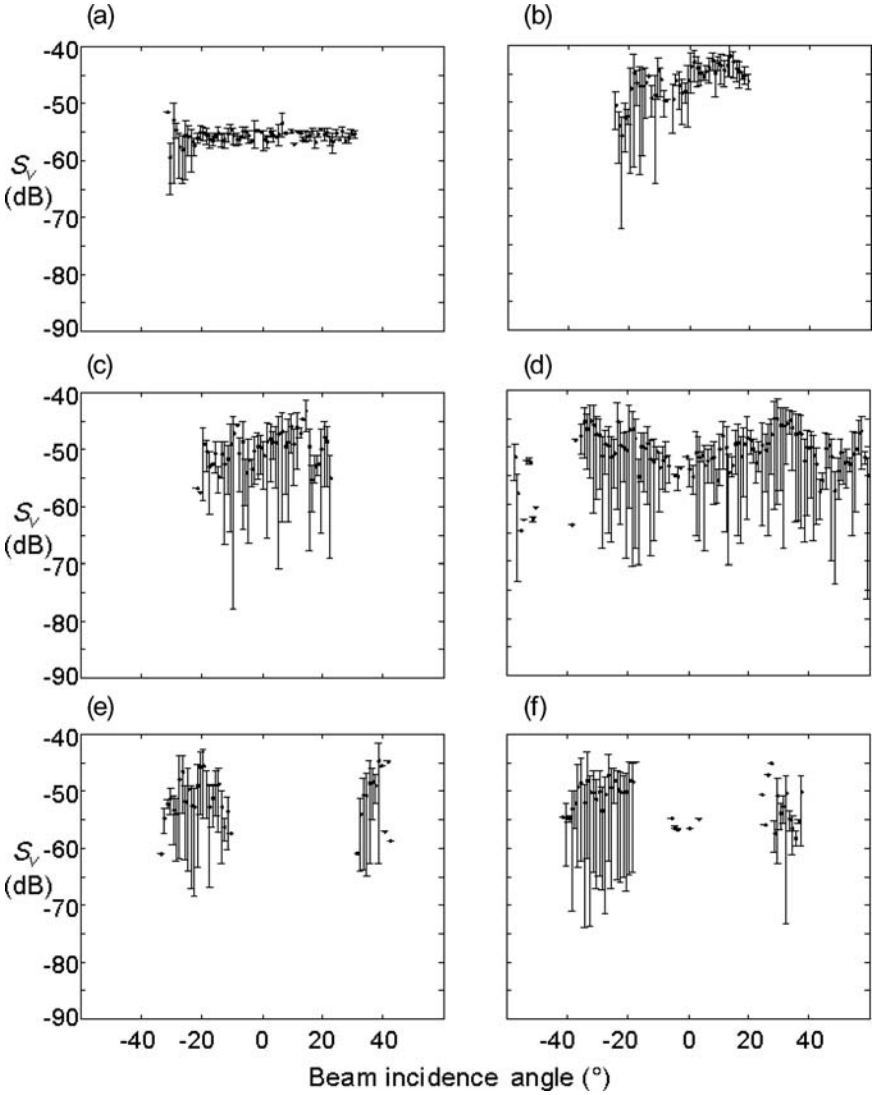

Figure 7. Measured S_v vs. beam direction from the 200 kHz MBE deployed in Antarctica. Examples of various patterns: (a) nearly uniform, (b) trending, (c) variable, (d) variable with diminished near-vertical incidence; in (e) and (f) there are no krill in the central, near-vertical beams.

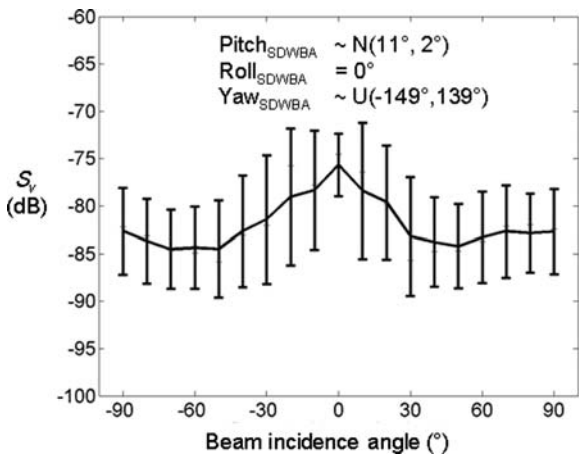

Figure 8. S_v vs. beam direction predicted by the SDWBA model for 200 kHz. Results for 25 krill per beam with pitch∼N(11°, 4°) and yaw∼U(−149°, 139°).

The complexities of high-frequency SDPs make it difficult to estimate krill-pitch distributions from measurements with a single-frequency MBE. In fact, the MBE measurements of S_v vs. beam direction in this study did not conform consistently to any of the simulation predictions. The simulations may be improved by accounting for additional factors, such as krill-length distributions and variations in their orientations within a swarm. In addition, the beam pattern, of the MBE should be taken into account. Either the simulated S_v should be convolved with the expected beam patterns, or the measured S_v should be deconvolved with the calibrated beam patterns. Future studies should include independent observations of krill orientation during acoustic surveys, perhaps using visual techniques.

Acknowledgements

We are grateful to Derek Needham and Mike Patterson (Sea Technology Services) for developing the MBE transducer-deployment apparatus, Steve Sessions (SWFSC) for adeptly driving the Zodiac inflatable boat in the often harsh conditions

of the Southern Ocean, and the UK National Environmental Research Council, Royal Society, and the US Antarctic Marine Living Resources Program for co-sponsoring the data-collection portion of this investigation. We thank Jeff Condiotty of Simrad, USA, for the use of the SM2000.

References

Chu, D., Foote, K. G., and Stanton, T. K. 1993. Further analysis of target-strength measurements of Antarctic krill at 38 and 120 kHz: comparison with deformed-cylinder model and inference of orientation distribution. Journal of the Acoustical Society of America, 93: 2985–2988.

Conti, S. G., and Demer, D. A. 2006. Improved parameterization of the SDWBA for estimating krill target strength. ICES Journal of Marine Science, 63: 928–935.

Conti, S. G., Demer, D. A., and Brierley, A. S. 2005. Broad-bandwidth, sound scattering, and absorption from krill (*Meganyctiphanes norvegica*), mysids (*Praunus flexuosus* and *Neomysis integer*), and shrimp (*Crangon crangon*). ICES Journal of Marine Science, 62: 956–965.

Cox, M. J., Demer, D. A., Warren, J. D., Cutter, G. R., and Brierley, A. S. Multibeam echosounder observations of Antarctic krill (*Euphausia superba*) swarms and interactions between krill and air breathing predators. Deep Sea Research II, in press.

Cutter, G. R., and Demer, D. A. 2007. Accounting for scattering directivity and fish behaviour in multibeam-echosounder surveys. ICES Journal of Marine Science, 64: 1664–1674.

Demer, D. A., and Conti, S. G. 2003a. Reconciling theoretical versus empirical target strengths of krill: effects of phase variability on the distorted-wave Born approximation. ICES Journal of Marine Science, 60: 429–434.

Demer, D. A., and Conti, S. G. 2003b. Validation of the stochastic distorted-wave Born approximation model with broad bandwidth total target strength measurements of Antarctic krill. ICES Journal of Marine Science, 60: 625–635.

Demer, A. D., and Conti, S. G. 2005. New target-strength model indicates more krill in the Southern Ocean. ICES Journal of Marine Science, 62: 25–32.

Endo, Y. 1993. Orientation of Antarctic krill in an aquarium. Nippon Suisan Gakkaishi, 59: 465–468.

Gerlotto, F., Castillo, J., Saavedra, A., Barbieri, M. A., Espejo, M., and Cotel, P. 2004. Three-dimensional structure and avoidance behaviour of anchovy and common sardine schools in central, southern Chile. ICES Journal of Marine Science, 61: 1120–1126.

Gerlotto, F., and Fréon, P. 1992. Some elements on vertical avoidance of fish schools to a vessel during acoustic surveys. Fisheries Research, 14: 251–259.

Jech, J. M., and Horne, J. K. 2002. Three-dimensional visualization of fish morphometry and acoustic backscatter. Acoustic Research Letters Online, 3(1): 35–40.

Kils, U. 1981. The swimming behaviour, swimming performance and energy balance of Antarctic krill *Euphausia superba*. BIOMASS Scientific Series, 3. 122 pp.

Lawson, G. L., Wiebe, P. H., Ashjian, C. J., Chu, D., and Stanton, T. K. 2006. Improved parameterization of Antarctic krill target-strength models. Journal of the Acoustical Society of America, 119: 232–242.

Martin Traykovski, L. V., O'Driscoll, R. L., and McGehee, D. E. 1998. Effect of orientation on broadband acoustic scattering of Antarctic krill *Euphausia superba*: implications for inverting zooplankton spectral acoustic signatures for angle of orientation. Journal of the Acoustical Society of America, 104: 2121–2135.

McGehee, D. E., O'Driscoll, R. L., and Martin Traykovski, L. V. 1998. Effects of orientation on acoustic scattering from Antarctic krill at 120 kHz. Deep Sea Research II, 45: 1273–1294.

Soria, M., Fréon, P., and Gerlotto, F. 1996. Analysis of vessel influence on spatial behaviour of fish schools using a multibeam sonar and consequences for biomass estimates by echosounder. ICES Journal of Marine Science, 53: 453–458.

Towler, R. H., Jech, J. M., and Horne, J. K. 2003. Visualizing fish movement, behaviour, and acoustic backscatter. Aquatic Living Resources, 16: 277–282.

doi:10.1093/icesjms/fsp040